



# HHS Public Access

Author manuscript

*Am J Surg Pathol.* Author manuscript; available in PMC 2023 September 01.

Published in final edited form as:

*Am J Surg Pathol.* 2022 September 01; 46(9): 1298–1308. doi:10.1097/PAS.0000000000001915.

## Recurrent *KAT6B/A::KANSL1* Fusions Characterize a Potentially Aggressive Uterine Sarcoma Morphologically Overlapping with Low-grade Endometrial Stromal Sarcoma

Abbas Agaimy, MD<sup>1</sup>, Blaise A. Clarke, MD<sup>2</sup>, David L. Kolin, MD<sup>3</sup>, Cheng-Han Lee, MD<sup>4</sup>, Jen-Chieh Lee, MD, PhD<sup>5</sup>, W Glenn McCluggage, FRCPath<sup>6</sup>, Patrik Pöschke, MD<sup>7</sup>, Robert Stoehr, PhD<sup>1</sup>, David Swanson, BSc<sup>8</sup>, Gulisa Turashvili, MD<sup>8,9</sup>, Matthias W. Beckmann, MD<sup>7</sup>, Arndt Hartmann, MD<sup>1</sup>, Cristina R. Antonescu, MD<sup>10</sup>, Brendan C. Dickson, MD, MSc<sup>8,9</sup>

<sup>1</sup>Institute of Pathology, Erlangen University Hospital, Comprehensive Cancer Center, European Metropolitan Area Erlangen-Nuremberg (CCC ER-EMN), Friedrich Alexander University of Erlangen-Nuremberg, Erlangen, Germany

<sup>2</sup>University Health Network, Toronto, ON, Canada

<sup>3</sup>Brigham and Woman's Hospital, Boston, MA, USA

<sup>4</sup>BC Cancer Agency, Vancouver, BC, Canada

<sup>5</sup>Department and Graduate Institute of Pathology, National Taiwan University Hospital, National Taiwan University College of Medicine, Taipei, Taiwan

<sup>6</sup>Department of Pathology, Belfast Health & Social Care Trust, Belfast, United Kingdom

<sup>7</sup>Department of Gynecology and Obstetrics, Erlangen University Hospital, Comprehensive Cancer Center, European Metropolitan Area Erlangen-Nuremberg (CCC ER-EMN), Friedrich Alexander University of Erlangen-Nuremberg, Erlangen, Germany

<sup>8</sup>Department of Pathology & Laboratory Medicine, Mount Sinai Hospital, Toronto, ON, Canada

<sup>9</sup>Department of Pathobiology and Laboratory Medicine, University of Toronto, Toronto, ON, Canada

<sup>10</sup>Department of Pathology, Memorial Sloan Kettering Cancer Center, New York, NY, USA

### Abstract

With the widespread application of next generation sequencing, the genetic landscape of uterine mesenchymal neoplasms has been evolving rapidly to include several recently identified fusion genes. Although chromosomal rearrangements involving the 10q22 and 17q21.31 loci have been reported in occasional uterine leiomyomas decades ago, the corresponding *KAT6B::KANSL1* fusion has been only recently identified in two uterine tumors diagnosed as leiomyoma and leiomyosarcoma. We herein describe 13 uterine stromal neoplasms carrying a *KAT6B::KANSL1*

---

Address page proofs, correspondence, and requests for reprints to Abbas Agaimy, MD, Pathologisches Institut, Universitätsklinikum Erlangen, Krankenhausstrasse 8-10, 91054 Erlangen, Germany, Phone: +49-9131-85-22288, Fax: +49-9131-85-24745, abbas.agaimy@uk-erlangen.de.

Conflict of interest: none

(n=11) and *KAT6A::KANS1* (n=2) fusion. Patient ages ranged from 33 to 81 years (median, 49). Tumor size was 2.6 – 23.5 cm (median, 8.2). Nine tumors were myometrium-centered and three had an intracavitary component. Original diagnoses were mostly low-grade endometrial stromal sarcoma (LG-ESS; 10 cases) with atypical features (limited CD10 expression, sex cord-like features, pericytic vasculature, and frequent myxoid changes). Treatment was hysterectomy +/- bilateral salpingo-oophorectomy (10), myomectomy (1) and curettage (2). Five patients were disease-free at 6 to 34 months, 3 (27%) died of disease at 2 to 47 months, and three were alive with disease at 2, 17 and 17 years. Histologically, most tumors showed variable overlap with LG-ESS, but they were generally well circumscribed lacking the extensive permeative and angioinvasive growth typical of LG-ESS. They were composed of monotonous medium-sized oval and spindle cells arranged into diffuse sheets with prominent spiral-type arterioles and frequent pericytoma-like vascular pattern. Variable myxoid stromal changes were frequent. Mitotic activity ranged from 1 to >20 in 10 HPFs. Immunohistochemistry showed variable expression of CD10 (12/13), ER (8/11), PR (8/11), smooth muscle actin (9/11), desmin (4/12), h-caldesmon (2/10), calretinin (3/8), inhibin (1/7), WT1 (4/7), cyclinD1 (5/11; diffuse in only one case) and pankeratin (5/10).

This series characterizes a *KAT6B/A::KANS1*-fusion positive uterine stromal neoplasm within the morphological spectrum of LG-ESS but with atypical features. The relationship of these neoplasms to genuine LG-ESS remains unclear. This molecular subtype of uterine ESS has the potential for an unfavorable clinical course despite absence of widely invasive growth; nevertheless, analysis of more cases is necessary to delineate the phenotypic spectrum and biological potential of this tumor.

### Keywords

low-grade endometrial stromal sarcoma; smooth muscle neoplasm; KAT6B; KAT6A; KANS1; uterus; sarcoma; leiomyoma

## INTRODUCTION

During the last two decades, significant progress has been made in elucidating the genetic landscape of uterine mesenchymal neoplasms, with delineation of novel entities and characterization of the molecular drivers in the spectrum of established neoplasms. Most of these recent advances concern identification of fusion genes.<sup>1-3</sup> In smooth muscle neoplasms, *PLAG1* and *PGR* fusions have been recognized as genetic drivers in subsets of leiomyosarcomas characterized by prominent myxoid and epithelioid/rhabdoid features, respectively.<sup>4-6</sup> *ALK* fusions have been confirmed in inflammatory myofibroblastic tumors.<sup>7-9</sup> In the spectrum of fibrosarcoma-like malignancies, a variety of recurrent fusions have allowed identification of distinct entities, including *NTRK*, *COL1A1::PDGFB*, and *RET* fusions.<sup>10,11</sup> Uterine tumors resembling ovarian sex cord stromal tumors (UTROSCT) represent another tumor with recently characterized recurrent fusion genes involving *ESR1*, *GREB1*, *NCOA1-3*, and others.<sup>12-14</sup>

The molecular landscape of uterine endometrial stromal neoplasms has emerged as well to include recurrent gene fusions in low-grade (LG-) and high-grade (HG-) endometrial

stromal sarcoma (ESS).<sup>2</sup> The *JAZF1::SUZ12* fusion characterizes the majority of LG-ESS, but many other variants (*JAZF1::BCORL1*, *MEAF6::SUZ12*, *EPC1::SUZ12*, *EPC1::BCOR* and others) have been reported recently.<sup>2,15–17</sup> On the other hand, the HG-ESS variant frequently harbors *YWHAE::NUTM2A/B*, *ZC3H7B::BCOR*, *LPP::BCOR* fusions or *BCOR* internal tandem duplications.<sup>18–20</sup>

Although chromosomal rearrangements involving the 10q22 and 17q21.31 loci have been reported in occasional uterine smooth muscle tumors decades ago<sup>21–23</sup>, the corresponding *KAT6B::KANS1* fusion has been only recently identified in two uterine tumors diagnosed as leiomyoma<sup>24</sup> and leiomyosarcoma.<sup>25</sup> In the current study, we expand the morphologic and genotypic spectrum of a novel uterine stromal neoplasm characterized by recurrent *KAT6B/A::KANS1* fusions. Given the evolving entity-specific guidelines for treatment and follow-up of patients with uterine sarcomas, it seems justified to correctly identify and precisely subtype these emerging tumors so that they can be better stratified for optimized therapy and follow-up strategies.<sup>26</sup>

## MATERIALS AND METHODS

Cases were identified in the consultation files of the authors (n=11) and in the routine files of the Pathology Department, Erlangen, Germany. The tissue specimens were fixed in formalin and processed routinely for histopathology. Due to the consultation nature of most of the cases, immunohistochemistry (IHC) was performed in different laboratories and the stains varied from case to case, based on tissue availability (details of the staining protocols and antibody sources are available upon request). Results of cyclin D1 immunostaining were assessed in a binary fashion as either diffuse or homogeneous (>70% of nuclei stained) or non-diffuse (variable or heterogeneous nuclear staining in <70% of cells).<sup>27</sup>

### Next generation sequencing

For Cases 1, 2, 3 and 13 (Table 1), RNA was isolated from formalin-fixed paraffin embedded (FFPE) tissue sections using RNeasy FFPE Kit of Qiagen (Hilden, Germany) and quantified spectrophotometrically using NanoDrop-1000 (Waltham, United States). Molecular analysis was performed using the TruSight RNA Fusion panel (Illumina, Inc., San Diego, CA, USA) with 500 ng RNA as input according to the manufacturer's protocol. Libraries were sequenced on a MiSeq (Illumina, Inc., San Diego, CA, USA) with > 3 million reads per case, and sequences were analyzed using the RNA-Seq Alignment workflow, version 2.0.1 (Illumina, Inc., San Diego, CA, USA). The Integrative Genomics Viewer (IGV), version 2.2.13 (Broad Institute, REF) was used for data visualization.<sup>28</sup>

Cases 4 to 9 were subjected to targeted RNA sequencing using Illumina RNA-Fusion assay as described previously.<sup>12</sup> The RNA from the FFPE tissue in Cases 10 and 12 was subjected to transcriptomic sequencing using the TruSeq RNA Exome kit (Illumina, San Diego, CA, USA) as previously reported.<sup>29</sup>

Fluorescence in-situ hybridization (FISH) was performed on Case 1, 2 and 3 on formalin-fixed paraffin-embedded 4 µm tissue sections using custom bacterial artificial chromosomes (BAC) flanking *KAT6A*, *KAT6B* and *KANS1* using the

methods described previously [30] (supplementary table). For case 10, reverse transcription polymerase chain reaction (RT-PCR) was conducted as previously described, using primer sets as follows: 5'-GAAAGACGGACCGCAGTACA-3' (forward primer, set 1), 5'-TGCAGCAACAGACATTGGGA-3' (reverse primer, set 1), 5'-TGGGAGCTTAGATGGCAAAGG-3' (forward primer, set 2), and 5'-TTCTCTACGCGAGTTGTTGC-3' (reverse primer, set 2).<sup>30</sup>

## RESULTS

### Clinical features

The main clinicopathological and demographic features are summarized in Table 1. Patient age ranged from 33 to 81 years (median, 49). All patients presented with non-specific symptoms indistinguishable from uterine fibroids. Nine patients received hysterectomy (three after initial enucleation/ myomectomy) with or without bilateral salpingo-oophorectomy. Two patients underwent curettage only. One patient received myomectomy for her primary tumor and total abdominal hysterectomy with bilateral salpingo-oophorectomy and debulking surgery for extensive local pelvic and peritoneal recurrence (7 years after diagnosis), followed by further surgeries for additional recurrences (1.5 and 8 years after 1<sup>st</sup> recurrence). She also received palliative chemoradiation and hormone therapy. Follow-up was available for 11 patients ranging 2 to 204 months (median, 23). Three patients (27%) died of disease at 2, 10, and 47 months after diagnosis; three were alive with persistent disease at 24, 204 and 204 months. One of the patient with long-term follow-up had persistent disease verified by curetting 17 years after initial curetting but exact status of her disease was unknown. The other patient developed multiple recurrences at 7, 8.5 and 17 years. Lung metastases were diagnosed synchronously in one patient and at 46 months in another. Five patients were alive without disease recurrence or metastases at 6, 9, 10, 17 and 34 months.

### Pathological findings

The major findings are summarized in (Table 2). Tumor size ranged from 2.6 – 23.5 cm (median, 8.2) when this information was available. All tumors but one were solitary. Nine tumors were myometrium-centered, while three had a variable intracavitary component and one had an exophytic component projecting from the uterine serosa (Case 13). One patient presented with a 7.5 cm myometrial nodule and another larger nodule (15 cm) within the broad ligament. Eight of 11 tumors were well circumscribed but non-encapsulated, lacking the permeative growth of LG-ESS (Fig. 1A, B). Four tumors had infiltrative borders with variable entrapment of myometrium (Fig. 1C, D), but only one (Case 13) showed classical permeative pattern of LG-ESS. Their histology was largely similar with minor variations from case to case. The tumor cells were small to medium-sized monomorphic rounded to ovoid or spindled with a small rim of pale-eosinophilic to clear cytoplasm with indistinctive cell borders (Fig. 2A–D). Spiral-like arterioles were seen at least focally in all cases and were most prominent near the myometrial border (Fig. 2A). Focal to diffuse myxoid stroma was also noted in 9 cases, frequently with abrupt transition between non-myxoid and myxoid areas (Fig. 3A, B). In the background of myxoid areas, prominent thin-walled vessels were seen with communicating (Fig. 3C) or hemangiopericytoma-like (Fig. 3D)

pattern. Six cases showed foci with prominent sex cord-like branching corded and trabecular arrangements (Fig. 4A, B). Brightly eosinophilic collagenous deposits of variable shape and amount were present within the background stroma of 8 cases (Fig. 4C, D). Lymphovascular invasion was present in two cases, one of which exhibited frankly pleomorphic sarcomatous features (Fig. 1C, D; Fig. 4E). Foci with moderately eosinophilic stained cells resembling smooth muscle cells were seen focally in 6 cases (Fig. 4F). The mitotic counts ranged 1 to >20 (median, 3) per 10 high-power fields (Fig. 2C, D). Areas of necrosis were present in 9 tumors and were extensive in one. In Case 5, the uterine nodule showed similar histology as other cases, while the larger broad ligament nodule was less differentiated suggesting tumor progression (both nodules showed same fusion indicating common origin, see molecular results below).

Immunohistochemistry (Table 3) showed expression of CD10 (12/13; Fig. 5A, B), ER (8/11; Fig. 5C), PR (8/11), and variably mostly limited smooth muscle actin (9/11; Fig. 5D), desmin (4/12), h-caldesmon (2/10), calretinin (3/8), inhibin (1/7), WT1 (nuclear; 4/7), and pankeratin (5/10). While variable heterogeneous expression of cyclin D1 was seen in 5/11 cases, diffuse expression (>70% of cells) was noted in only one case.

### Molecular results

RNA sequencing revealed *KAT6B::KANSLI* fusion in 11 cases and a novel *KAT6A::KANSLI* fusion in two tumors (Table 4; Fig. 6). Eight *KAT6B*-rearranged tumors contained an exon 3 (of 18) fusion and two contained an exon 4 (of 18) fusion to *KANSLI* (exon 11 of 15). In Case 5, the two tumor nodules were tested separately; both showed same *KAT6B::KANSLI* fusion. Two tumors had a *KAT6A::KANSLI* fusion between exon 2 of *KAT6A* to exon 11 of *KANSLI*. Case 1, 2 and 3 were tested also by FISH, which confirmed the presence of *KAT6A*, *KAT6B* and *KANSLI* rearrangements (Fig. 7A, B). The fusion junction in Case 10 was validated with RT-PCR (Fig. 7C).

### DISCUSSION

Lysine Acetyltransferase 6B (*KAT6B*; earlier named the monocytic leukemia zinc finger protein-related factor or MORF) is a member of the MYST family of histone acetyltransferase, and maps to chromosomal region 10q22.<sup>31</sup> *KAT6A* is another member of the histone acetyltransferase family, mapping to 8p11.21.<sup>32</sup> These proteins influence the accessibility of DNA to transcription factors and are hence involved in the regulation of transcription and the cell cycle control.<sup>33</sup> Rearrangements involving *KAT6B* and *KAT6A* have been reported in a subset of acute leukemia, but they are very rare in solid tumors.<sup>34–36</sup>

*KAT8* Regulatory non-specific lethal Complex Subunit 1 (*KANSLI*) maps to 17q21.31 and is an evolutionarily highly conserved protein.<sup>37</sup> Mutations in *KANSLI* have been established as responsible for the 17q21.31 microdeletion syndrome.<sup>37</sup> Gene fusions of *KANSLI* have been reported in hematological malignancies, but involvement in solid tumors is exceptionally rare.<sup>38,39</sup>

Until recently, the role of the histone acetyltransferase family members *KAT6B* (10q22) and *KAT6A* (8p11.21), and the *KANSLI* gene (17q21.31), in the pathogenesis of uterine

mesenchymal neoplasms remained poorly understood. In 1988, Dal Cin *et al.* reported a t(10;17)(q22.1;p13) translocation in a cellular highly mitotically active uterine neoplasm with focal epithelioid features in a 39-year-old female.<sup>21</sup> Morphologically, this neoplasm showed fascicles of spindle cells along with whorls of cells surrounding prominent small vessels; moreover, the report described distinct epithelial areas. A few years later, in 1993, Ozisik *et al.* detected 10q22 rearrangements in eight conventional and one cellular uterine leiomyoma but no recurrent translocation partner was detected.<sup>22</sup> The 10q22-rearranged tumors represented 5% of all chromosomally abnormal leiomyomas in that study<sup>22</sup>; regrettably, this report did not include clinical or pathologic descriptions of these tumors.

In a cytogenetic study in 2004, Moore *et al.* reported recurrent chromosomal rearrangements involving 10q22 in four tumors described as uterine leiomyomas, two of which were cellular.<sup>23</sup> The authors identified *KAT6B* (*MORF*) as corresponding to the 10q22 rearrangement, but the fusion partner remained elusive.<sup>23</sup> They found that the *KAT6B* breakpoints in uterine tumors were distinct from those reported in acute myeloid leukemia.<sup>23,32</sup> Although three of their four cases showed recurrent involvement of 17q21 – in retrospect compatible with a *KAT6B::KANS1* fusion – the partner gene remained unknown at that time.<sup>23</sup>

Aside from these early cytogenetic studies, which lacked detailed histopathologic descriptions, the *KAT6B::KANS1* fusion has only recently been reported in three neoplasms: a retroperitoneal leiomyoma<sup>40</sup>, a cellular uterine leiomyoma<sup>24</sup> and a uterine leiomyosarcoma.<sup>25</sup> The tumor reported by Panagopoulos *et al.* in a 45 year-old woman was a large retroperitoneal mass. Morphologically unusual, this was a hypocellular spindle-stellate cell neoplasm with prominent loose fibromyxoid stroma.<sup>40</sup> The tumor cells expressed desmin, smooth muscle actin, estrogen receptor, and progesterone receptor. However, h-caldesmon and CD10 were not reported. The patient remained disease-free 4 years later. The second case, reported by Ainsworth *et al.*, comprised a rapidly growing uterine mass carrying the same fusion.<sup>24</sup> Morphologically striking, and bearing overlap with some of the cases in our cohort, this tumor was cellular and composed of fascicles of spindle cells interrupted by thick-walled vessels or fibrous regions. The tumor expressed desmin and h-caldesmon, along with strong patchy immunoreactivity to CD10. The patient was disease-free six months after hysterectomy [24]. The third case was a uterine “leiomyosarcoma” harboring a *KAT6B::KANS1* fusion included in the TCGA cohort (TCGA-HS-A5N8).<sup>25</sup> *KAT6A* has been only very rarely reported as a fusion partner in cancer; reported in a case of acute myeloid leukemia carrying a *KAT6A::CREBBP* fusion<sup>35</sup> and in a renal cell carcinoma carrying a *KAT6A::TFE3* fusion.<sup>36</sup> The *KAT6A::KANS1* fusion detected in two of our cases is novel.

The tumors reported in the current study frequently showed morphologic and immunophenotypic overlap with LG-ESS, a subset of which appeared to show sex cord-like differentiation. In addition, some of the tumors had myoid cell features. Notably, most, but not all, tumors had well-defined borders at their myometrial interface, while four tumors displayed variable (mostly subtle) myoinvasive growth including one tumor with the characteristic multinodular plexiform infiltrating pattern and/or the extensive intravascular permeation within the myometrium seen in the majority of LG-ESS.<sup>41,42</sup> The overall



appearance showed variability in cell morphology (ovoid to spindle cells), architecture (solid sheets, variable storiforming, and/ sex cord-like patterns) and stroma (variable fibromyxoid features with pericytoma-like vasculature). Likewise, the immunoprofile was not as consistent as in conventional LG-ESS. The frequent presence of myxoid features in our cohort is notable as is the presence of brisk mitotic activity in many cases. One tumor lacked CD10 expression but otherwise had a LG-ESS-compatible morphology. The lack of WT1 reactivity in many of these tumors represents another unusual feature when compared to conventional LG-ESS. Likewise, homogeneous expression of cyclinD1, seen in one case, is a consistent feature of HG-ESS and is unexpected in LG-ESS.<sup>27</sup> A subset of our cases showed frequent, albeit variable, immunoreactivity for smooth muscle actin and less frequently desmin; it is conceivable that this feature in conjunction with focal myoid cell appearance might be responsible for misattributing a subset of cases as leiomyoma or leiomyosarcoma in the past.<sup>21–25,40</sup> Moreover, a diagnosis of leiomyoma, STUMP or leiomyosarcoma was considered originally in some of our cases. However, with the exception of variable moderate cytoplasmic eosinophilia, the tumor cells did not show classical cytological (larger elongated cells with fibrillary eosinophilic cytoplasm), nuclear (blunt-ending cigar-shaped nuclei), or architectural (compact intersecting fascicles) features of smooth muscle cells. While the 13 cases in our cohort share significant overlap with LG-ESS, it is presently unclear whether these tumors are in fact related; this is highlighted by a fact that most cases appeared to be myometrial based. Furthermore, given that one tumor reportedly in the literature arose outside of the uterus<sup>40</sup>, it remains unclear whether these tumors are limited to the uterus.

In view of the well-known morphologic heterogeneity in conventional LG-ESS, it is conceivable the current cases reflect a molecular subtype of LG-ESS. Nevertheless, the absence of genetic overlap to date, combined with several, albeit in part subtle, morphologic differences, raises the possibility these neoplasms represent potentially a distinct entity with morphologic and immunophenotypic overlap with LG-ESS and smooth muscle neoplasms. It is conceivable that with larger cohorts, and more in-depth study with gene expression and/or methylation profiling studies, these issues will be resolved in the future.

Although many tumors in our series showed brisk mitotic activity and variation in cellularity suggesting high-grade transformation<sup>43</sup>, no recognizable transition from low-grade to high-grade areas was noted and the mitotic activity was similarly high in those less cellular tumor areas with prominence of spiral and thick-walled arterioles, especially at the myometrial interface. The fact that 27% of patients died of their disease at a median of 10 months suggests a biologic potential warranting designation as sarcoma. Based on the information available to date, we have tentatively labelled these neoplasms, which appears to have a striking predilection for the gynecologic tract, 'endometrial stromal sarcoma with *KAT6B/A::KANSL1* rearrangement'.

Recognizing potential cases in routine clinical practice may pose true challenges in laboratories without access to or with only rare use of molecular profiling. Based on the findings in our current cases and given the potentially malignant clinical behavior associated with the *KAT6B/A::KANSL1* fusions, we believe that circumscribed uterine tumors exhibiting mixed endometrial stromal (classic or fibromyxoid variant) and smooth

muscle features or showing prominent hemangiopericytomatous vascular pattern should be considered for molecular testing. In particular, large uterine stromal neoplasms showing features of LG-ESS but lacking invasive permeative growth of LG-ESS should be considered for analysis. Criteria to distinguish between these two prognostically significantly different entities have to be established. Moreover, in the setting of large retroperitoneal gynecologic type tumors, we would also recommend molecular testing for tumors exhibiting similar features to our current series. However, it is important to note that this recommendation is based on the series described herein and there may be an inherent bias towards testing tumors with unusual histologic features which may consequently be associated with more aggressive clinical behavior. Additional studies are needed to fully delineate the frequency, and the histologic and clinical spectrum of uterine and extrauterine tumors harboring *KAT6B/A::KANSL1* fusions.

## Supplementary Material

Refer to Web version on PubMed Central for supplementary material.

## Funding:

P50 CA 140146-01 (CRA), P50 CA217694 (CRA), P30 CA008748 (CRA). This work was also in part supported by the research fund from the Ministry of Science and Technology, Taiwan (MOST 109-2326-B-002-010-MY3) to Dr. Jen-Chieh Lee.

## REFERENCES

1. Rommel B, Holzmann C, Bullerdiek J. Malignant mesenchymal tumors of the uterus - time to advocate a genetic classification. *Expert Rev Anticancer Ther* 2016;16:1155–1166. [PubMed: 27602604]
2. Ferreira J, Félix A, Lennerz JK, Oliva E. Recent advances in the histological and molecular classification of endometrial stromal neoplasms. *Virchows Arch* 2018;473:665–678. [PubMed: 30324234]
3. Momeni-Boroujeni A, Chiang S. Uterine mesenchymal tumours: recent advances. *Histopathology* 2020;76:64–75. [PubMed: 31846533]
4. Chiang S Recent advances in smooth muscle tumors with PGR and PLAG1 gene fusions and myofibroblastic uterine neoplasms. *Genes Chromosomes Cancer* 2021;60:138–146. [PubMed: 33230916]
5. Arias-Stella JA 3rd, Benayed R, Oliva E, Young RH, Hoang LN, Lee CH, Jungbluth AA, Frosina D, Soslow RA, Antonescu CR, Ladanyi M, Chiang S. Novel PLAG1 Gene Rearrangement Distinguishes a Subset of Uterine Myxoid Leiomyosarcoma From Other Uterine Myxoid Mesenchymal Tumors. *Am J Surg Pathol* 2019;43:382–388. [PubMed: 30489320]
6. Chiang S, Samore W, Zhang L, Sung YS, Turashvili G, Murali R, Soslow RA, Hensley ML, Swanson D, Dickson BC, Stewart CJR, Oliva E, Antonescu CR. PGR Gene Fusions Identify a Molecular Subset of Uterine Epithelioid Leiomyosarcoma With Rhabdoid Features. *Am J Surg Pathol* 2019;43:810–818. [PubMed: 30829727]
7. Haimes JD, Stewart CJR, Kudlow BA, Culver BP, Meng B, Koay E, Whitehouse A, Cope N, Lee JC, Ng T, McCluggage WG, Lee CH. Uterine Inflammatory Myofibroblastic Tumors Frequently Harbor ALK Fusions With IGFBP5 and THBS1. *Am J Surg Pathol* 2017;41:773–780. [PubMed: 28490045]
8. Bennett JA, Nardi V, Rouzbahman M, Morales-Oyarvide V, Nielsen GP, Oliva E. Inflammatory myofibroblastic tumor of the uterus: a clinicopathological, immunohistochemical, and molecular analysis of 13 cases highlighting their broad morphologic spectrum. *Mod Pathol* 2017;30:1489–1503. [PubMed: 28664932]

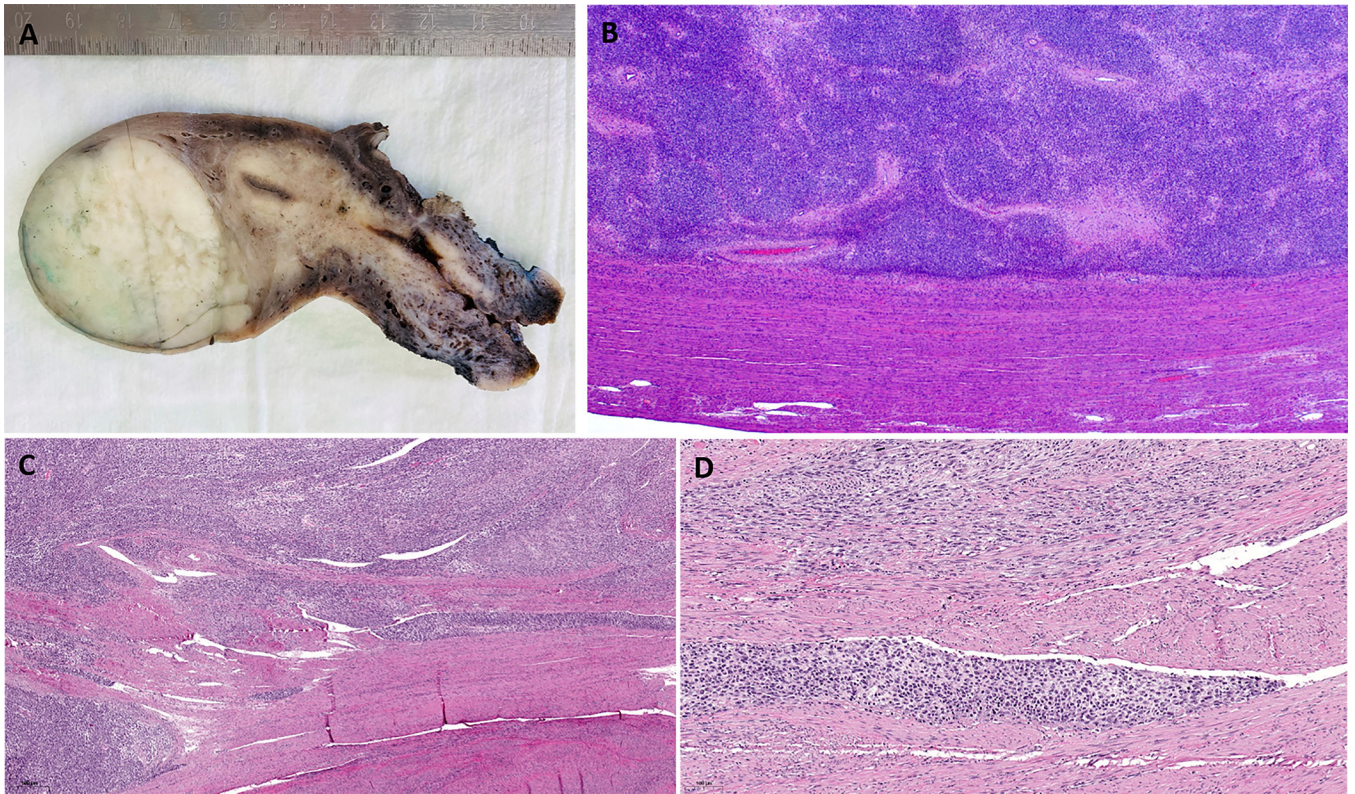


9. Ptáková N, Miesbauerová M, Kos un J, Grossmann P, Šidlová H, Pavelka J, Presl J, Alaghehbandan R, Bouda J, Ondi O. Immunohistochemical and selected genetic reflex testing of all uterine leiomyosarcomas and STUMPs for ALK gene rearrangement may provide an effective screening tool in identifying uterine ALK-rearranged mesenchymal tumors. *Virchows Arch* 2018;473:583–590. [PubMed: 30116888]
10. Croce S, Hostein I, Longacre TA, Mills AM, Pérot G, Devouassoux-Shisheboran M, Velasco V, Floquet A, Guyon F, Chakiba C, Querleu D, Khalifa E, Mayeur L, Rebier F, Leguellec S, Soubeyran I, McCluggage WG. Uterine and vaginal sarcomas resembling fibrosarcoma: a clinicopathological and molecular analysis of 13 cases showing common NTRK-rearrangements and the description of a COL1A1-PDGFB fusion novel to uterine neoplasms. *Mod Pathol* 2019;32:1008–1022. [PubMed: 30877273]
11. Croce S, Hostein I, McCluggage WG. NTRK and other recently described kinase fusion positive uterine sarcomas: A review of a group of rare neoplasms. *Genes Chromosomes Cancer* 2021;60:147–159. [PubMed: 33099837]
12. Dickson BC, Childs TJ, Colgan TJ, Sung YS, Swanson D, Zhang L, Antonescu CR. Uterine Tumor Resembling Ovarian Sex Cord Tumor: A Distinct Entity Characterized by Recurrent NCOA2/3 Gene Fusions. *Am J Surg Pathol* 2019;43:178–186. [PubMed: 30273195]
13. Goebel EA, Hernandez Bonilla S, Dong F, Dickson BC, Hoang LN, Hardisson D, Lacambra MD, Lu FI, Fletcher CDM, Crum CP, Antonescu CR, Nucci MR, Kolin DL. Uterine Tumor Resembling Ovarian Sex Cord Tumor (UTROSCT): A Morphologic and Molecular Study of 26 Cases Confirms Recurrent NCOA1–3 Rearrangement. *Am J Surg Pathol* 2020;44:30–42. [PubMed: 31464709]
14. Kao YC, Lee JC. An update of molecular findings in uterine tumor resembling ovarian sex cord tumor and GREB1-rearranged uterine sarcoma with variable sex-cord differentiation. *Genes Chromosomes Cancer* 2021;60:180–189. [PubMed: 33099842]
15. Huang HY, Ladanyi M, Soslow RA. Molecular detection of JAZF1-JJAZ1 gene fusion in endometrial stromal neoplasms with classic and variant histology: evidence for genetic heterogeneity. *Am J Surg Pathol* 2004;28:224–32. [PubMed: 15043312]
16. Lin DI, Huang RSP, Mata DA, Decker B, Danziger N, Lechpammer M, Hiemenz M, Ramkissoon SH, Ross JS, Elvin JA. Clinicopathological and genomic characterization of BCORL1-driven high-grade endometrial stromal sarcomas. *Mod Pathol* 2021;34:2200–2210. [PubMed: 34302054]
17. Dickson BC, Lum A, Swanson D, Bernardini MQ, Colgan TJ, Shaw PA, Yip S, Lee CH. Novel EPC1 gene fusions in endometrial stromal sarcoma. *Genes Chromosomes Cancer* 2018;57:598–603. [PubMed: 30144186]
18. Lee CH, Mariño-Enriquez A, Ou W, Zhu M, Ali RH, Chiang S, Amant F, Gilks CB, van de Rijn M, Oliva E, Debiec-Rychter M, Dal Cin P, Fletcher JA, Nucci MR. The clinicopathologic features of YWHAE-FAM22 endometrial stromal sarcomas: a histologically high-grade and clinically aggressive tumor. *Am J Surg Pathol* 2012;36:641–53. [PubMed: 22456610]
19. Mariño-Enriquez A, Lauria A, Przybyl J, Ng TL, Kowalewska M, Debiec-Rychter M, Ganesan R, Sumathi V, George S, McCluggage WG, Nucci MR, Lee CH, Fletcher JA. BCOR Internal Tandem Duplication in High-grade Uterine Sarcomas. *Am J Surg Pathol* 2018;42:335–341. [PubMed: 29200103]
20. Lewis N, Soslow RA, Delair DF, Park KJ, Murali R, Hollmann TJ, Davidson B, Micci F, Panagopoulos I, Hoang LN, Arias-Stella JA 3rd, Oliva E, Young RH, Hensley ML, Leitao MM Jr, Hameed M, Benayed R, Ladanyi M, Frosina D, Jungbluth AA, Antonescu CR, Chiang S. ZC3H7B-BCOR high-grade endometrial stromal sarcomas: a report of 17 cases of a newly defined entity. *Mod Pathol* 2018;31:674–684. [PubMed: 29192652]
21. Dal Cin P, Boghosian L, Crickard K, Sandberg AA. t(10;17) as the sole chromosome change in a uterine leiomyosarcoma. *Cancer Genet Cytogenet* 1988;32:263–6. [PubMed: 3163264]
22. Ozisik YY, Meloni AM, Surti U, Sandberg AA. Involvement of 10q22 in leiomyoma. *Cancer Genet Cytogenet* 1993;69:132–5. [PubMed: 8402551]
23. Moore SD, Herrick SR, Ince TA, Kleinman MS, Dal Cin P, Morton CC, Quade BJ. Uterine leiomyomata with t(10;17) disrupt the histone acetyltransferase MORF. *Cancer Res* 2004;64:5570–7.

24. Ainsworth AJ, Dashti NK, Mounajjed T, Fritchie KJ, Davila J, Mopuri R, Jackson RA, Halling KC, Bakkum-Gamez JN, Schoolmeester JK. Leiomyoma with KAT6B-KANSL1 fusion: case report of a rapidly enlarging uterine mass in a postmenopausal woman. *Diagn Pathol* 2019;14:32. [PubMed: 31027501]
25. Choi J, Manzano A, Dong W, Bellone S, Bonazzoli E, Zammataro L, Yao X, Deshpande A, Zaidi S, Guglielmi A, Gnutti B, Nagarkatti N, Tymon-Rosario JR, Harold J, Mauricio D, Zeybek B, Menderes G, Altwerger G, Jeong K, Zhao S, Buza N, Hui P, Ravaggi A, Bignotti E, Romani C, Todeschini P, Zanotti L, Odicino F, Pecorelli S, Ardighieri L, Bilguvar K, Quick CM, Silasi DA, Huang GS, Andikyan V, Clark M, Ratner E, Azodi M, Imielinski M, Schwartz PE, Alexandrov LB, Lifton RP, Schlessinger J, Santin AD. Integrated mutational landscape analysis of uterine leiomyosarcomas. *Proc Natl Acad Sci U S A*. 2021;118:e2025182118. [PubMed: 33876771]
26. Denschlag D, Thiel FC, Ackermann S, Harter P, Juhasz-Boess I, Mallmann P, Strauss HG, Ulrich U, Horn LC, Schmidt D, Vordermark D, Vogl T, Reichardt P, Gaß P, Gebhardt M, Beckmann MW. Sarcoma of the Uterus. Guideline of the DGGG (S2k-Level, AWMF Registry No. 015/074, August 2015). *Geburtshilfe Frauenheilkd*. 2015;75:1028–1042. [PubMed: 26640293]
27. Lee CH, Ali RH, Rouzbahman M, Marino-Enriquez A, Zhu M, Guo X, Brunner AL, Chiang S, Leung S, Nelnyk N, Huntsman DG, Blake Gilks C, Nielsen TO, Dal Cin P, van de Rijn M, Oliva E, Fletcher JA, Nucci MR. Cyclin D1 as a diagnostic immunomarker for endometrial stromal sarcoma with YWHAE-FAM22 rearrangement. *Am J Surg Pathol* 2012;36:1562–70. [PubMed: 22982899]
28. Robinson JT, Thorvaldsdóttir H, Winckler W, Guttman M, Lander ES, Getz G, Mesirov JP. Integrative Genomics Viewer. *Nature Biotechnology* 2011;29:24–26.
29. Lee CH, Kao YC, Lee WR, Hsiao YW, Lu TP, Chu CY, Lin YJ, Huang HY, Hsieh TH, Liu YR, Liang CW, Chen TW, Yip S, Lum A, Kuo KT, Jeng YM, Yu SC, Chung YC, Lee JC. Clinicopathologic Characterization of GREB1-rearranged Uterine Sarcomas With Variable Sex-Cord Differentiation. *Am J Surg Pathol* 2019;43:928–942. [PubMed: 31094921]
30. Antonescu CR, Zhang L, Chang NE, Pawel BR, Travis W, Katabi N, Edelman M, Rosenberg AE, Nielsen GP, Dal Cin P, Fletcher CD. EWSR1-POU5F1 fusion in soft tissue myoepithelial tumors. A molecular analysis of sixty-six cases, including soft tissue, bone, and visceral lesions, showing common involvement of the EWSR1 gene. *Genes Chromosomes Cancer*. 2010 Dec;49(12):1114–24. [PubMed: 20815032]
31. Champagne N, Bertos NR, Pelletier N, Wang AH, Vezmar M, Yang Y, Heng HH, Yang XJ. Identification of a human histone acetyltransferase related to monocytic leukemia zinc finger protein. *J Biol Chem* 1999;274:28528–36. [PubMed: 10497217]
32. Borrow J, Stanton VP Jr, Andresen JM, Becher R, Behm FG, Chaganti RS, Civin CI, Disteche C, Dubé I, Frischauf AM, Horsman D, Mitelman F, Volinia S, Watmore AE, Housman DE. The translocation t(8;16)(p11;p13) of acute myeloid leukaemia fuses a putative acetyltransferase to the CREB-binding protein. *Nat Genet* 1996;14:33–41. [PubMed: 8782817]
33. Sterner DE, Berger SL. Acetylation of histones and transcription-related factors. *Microbiol Mol Biol Rev* 2000;64:435–59. [PubMed: 10839822]
34. Camós M, Esteve J, Jares P, Colomer D, Rozman M, Villamor N, Costa D, Carrió A, Nomdedéu J, Monserrat E, Campo E. Gene expression profiling of acute myeloid leukemia with translocation t(8;16)(p11;p13) and MYST3-CREBBP rearrangement reveals a distinctive signature with a specific pattern of HOX gene expression. *Cancer Res* 2006;66:6947–54. [PubMed: 16849538]
35. Panagopoulos I, Torkildsen S, Gorunova L, Tierens A, Tjønnfjord GE, Heim S. Comparison between karyotyping-FISH-reverse transcription PCR and RNA-sequencing-fusion gene identification programs in the detection of KAT6A-CREBBP in acute myeloid leukemia. *PLoS One* 2014;9:e96570. [PubMed: 24798186]
36. Pei J, Cooper H, Flieder DB, Talarchek JN, Al-Saleem T, Uzzo RG, Dulaimi E, Patchefsky AS, Testa JR, Wei S. NEAT1-TFE3 and KAT6A-TFE3 renal cell carcinomas, new members of MiT family translocation renal cell carcinoma. *Mod Pathol* 2019;32:710–716. [PubMed: 30622287]
37. Zollino M, Orteschi D, Murdolo M, Lattante S, Battaglia D, Stefanini C, Mercuri E, Chiurazzi P, Neri G, Marangi G. Mutations in KANSL1 cause the 17q21.31 microdeletion syndrome phenotype. *Nat Genet* 2012;44:636–8. [PubMed: 22544367]

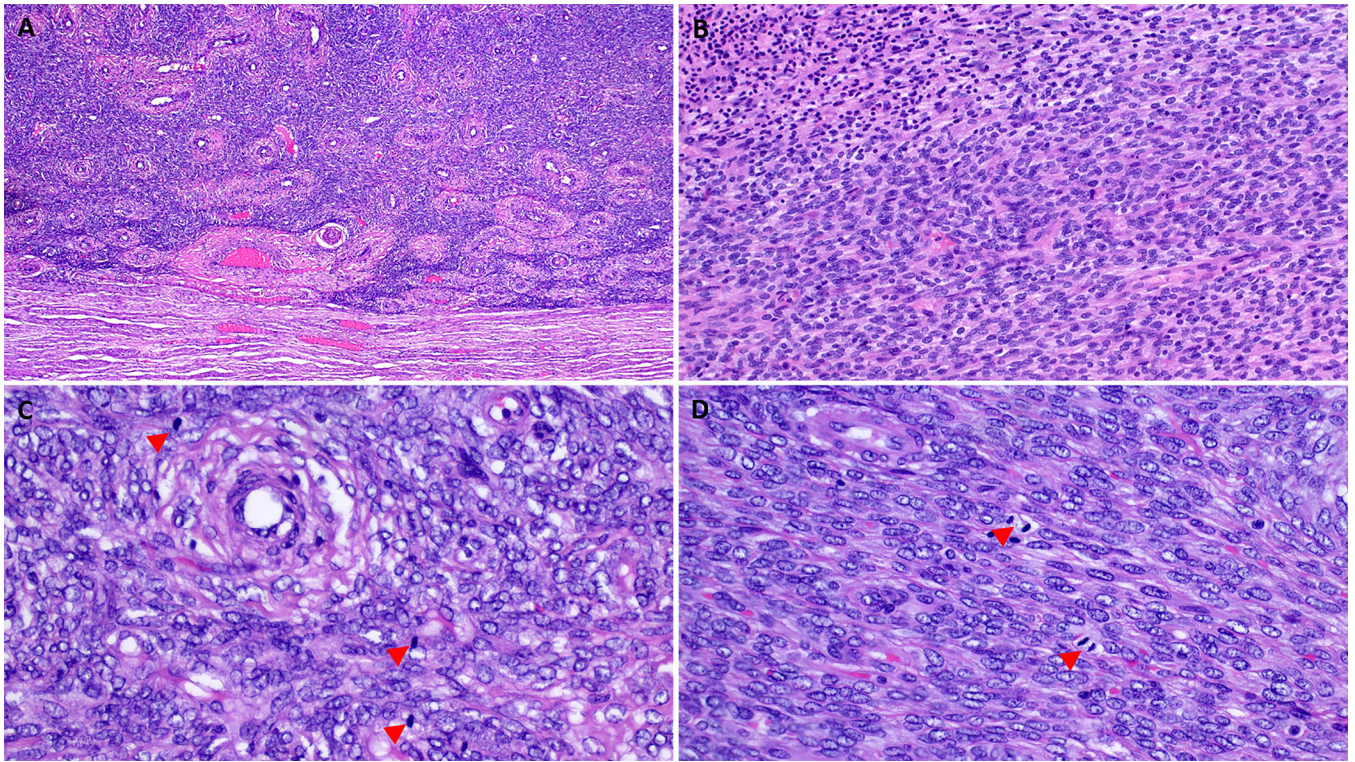
38. López-Nieva P, Fernández-Navarro P, Graña-Castro O, Andrés-León E, Santos J, Villa-Morales M, Cobos-Fernández MÁ, González-Sánchez L, Malumbres M, Salazar-Roa M, Fernández-Piqueras J. Detection of novel fusion-transcripts by RNA-Seq in T-cell lymphoblastic lymphoma. *Sci Rep* 2019;9:5179. [PubMed: 30914738]
39. Molony P, Smith AC, Selvarajah S, Sakhdari A. MDS/MPN-Unclassifiable with t(X;17)(q28;q21) and KANSL1-MTCP1/CMC4 Fusion Gene. *Cytogenet Genome Res* 2022:1–5.
40. Panagopoulos I, Gorunova L, Bjerkehagen B, Heim S. Novel KAT6B-KANSL1 fusion gene identified by RNA sequencing in retroperitoneal leiomyoma with t(10;17)(q22;q21). *PLoS One* 2015;10:e0117010. [PubMed: 25621995]
41. Chang KL, Crabtree GS, Lim-Tan SK, Kempson RL, Hendrickson MR. Primary uterine endometrial stromal neoplasms. A clinicopathologic study of 117 cases. *Am J Surg Pathol* 1990;14:415–38. [PubMed: 2327549]
42. Dionigi A, Oliva E, Clement PB, Young RH. Endometrial stromal nodules and endometrial stromal tumors with limited infiltration: a clinicopathologic study of 50 cases. *Am J Surg Pathol* 2002;26:567–81. [PubMed: 11979087]
43. Zou Y, Turashvili G, Soslow RA, Park KJ, Croce S, McCluggage WG, Stewart CJR, Oda Y, Oliva E, Young RH, Da Cruz Paula A, Dessources K, Ashley CW, Hensley ML, Yip S, Weigelt B, Benayed R, Antonescu CR, Lee CH, Chiang S. High-grade transformation of low-grade endometrial stromal sarcomas lacking YWHAE and BCOR genetic abnormalities. *Mod Pathol* 2020;33:1861–1870. [PubMed: 32317704]



**FIGURE 1.**

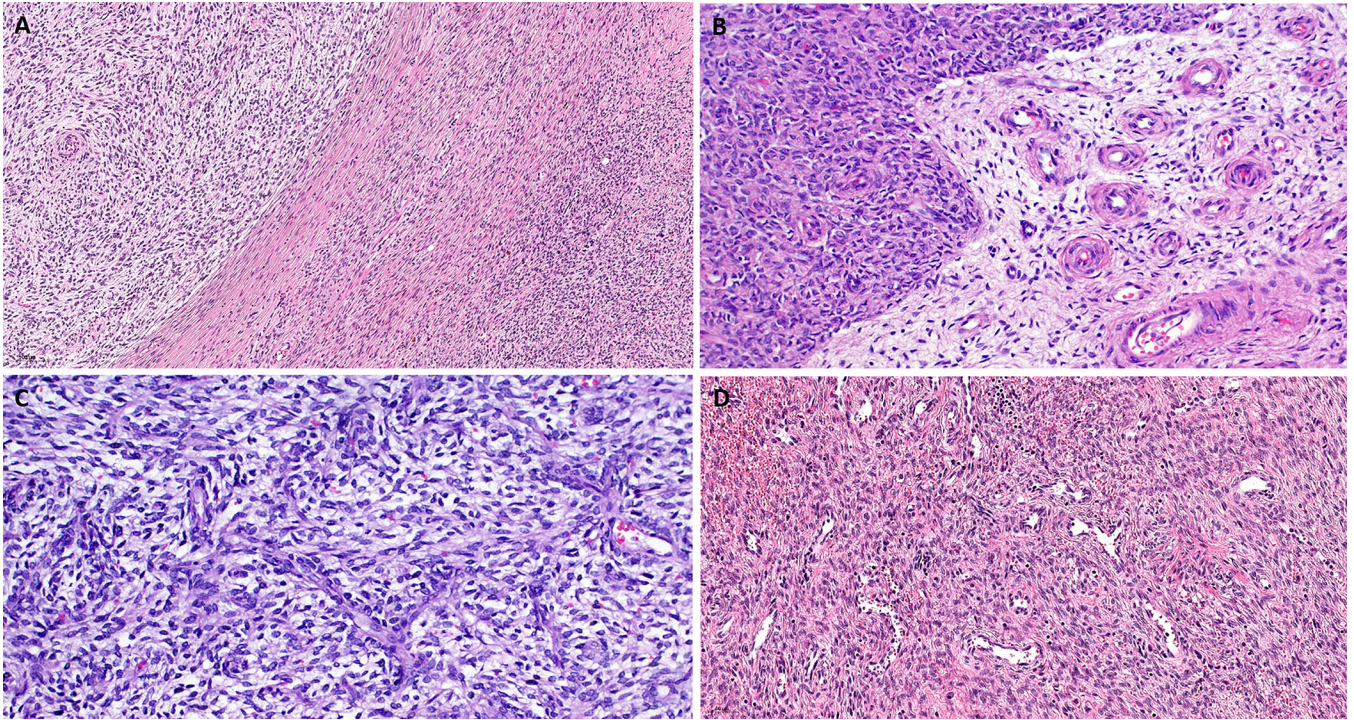
Representative examples of the gross and low-power features of *KAT6B::KANS1* fusion sarcomas. **A:** Gross image showing homogeneously tan-colored well-circumscribed nodule with subtle peripheral lobulation confined to the myometrium. **B:** Low power of same case highlights well-defined non-infiltrative borders at the myometrial interphase. **C:** This case showed myoinvasive borders akin to conventional LG-ESS. **D:** Tongue-like vascular permeation in same case.



**FIGURE 2.**

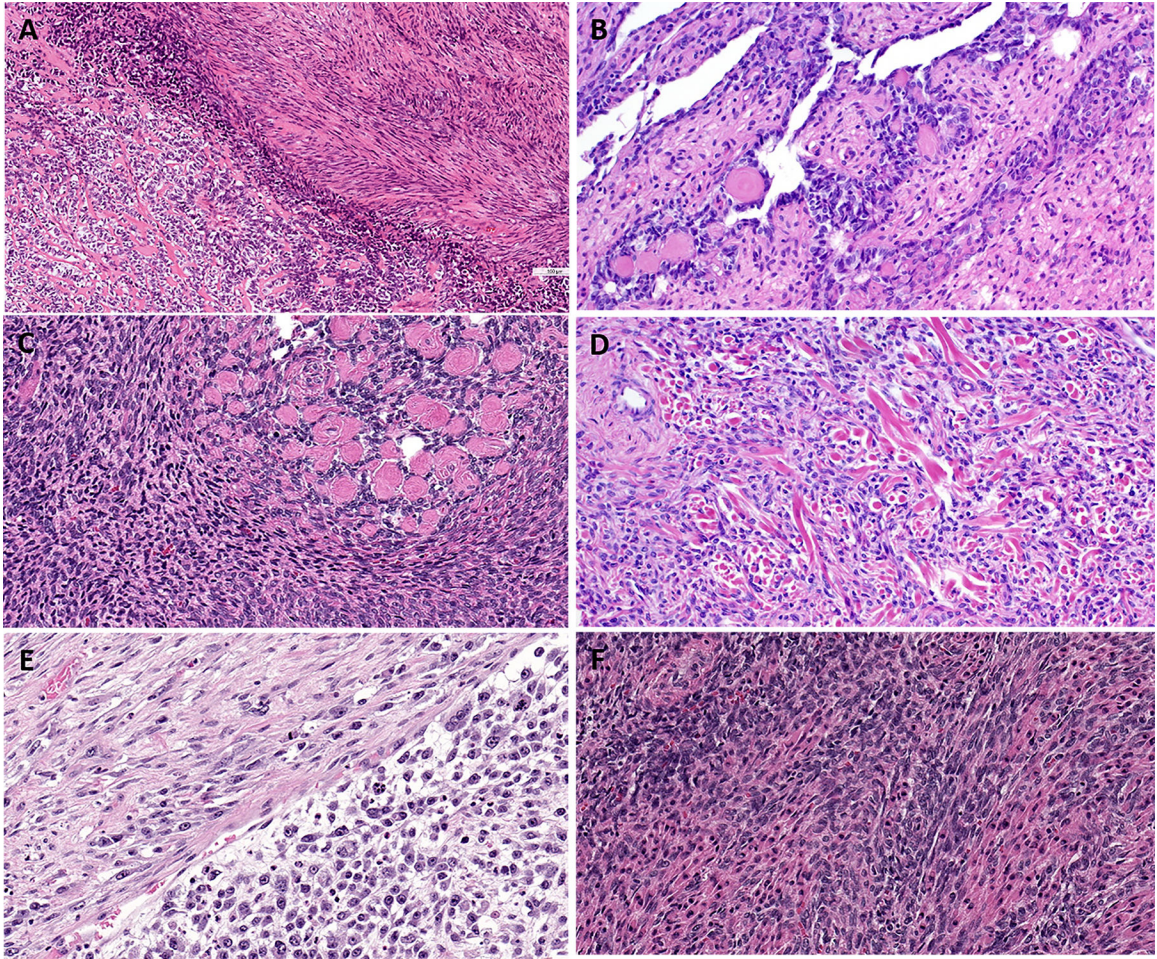
Examples of the common histological features of *KAT6B::KANS1* fusion sarcomas. **A:** LG-ESS-like pattern with prominent spiral-type arterioles is seen in particular near the myometrium. **B:** Cellular areas with ovoid to spindled cells, note necrosis (upper left field). **C:** Brisk mitotic activity is seen also in the low-grade looking areas in mitotically highly active tumors (arrow heads). **D:** Fibrosarcoma-like spindle cell pattern with brisk mitotic activity (arrow heads).



**FIGURE 3.**

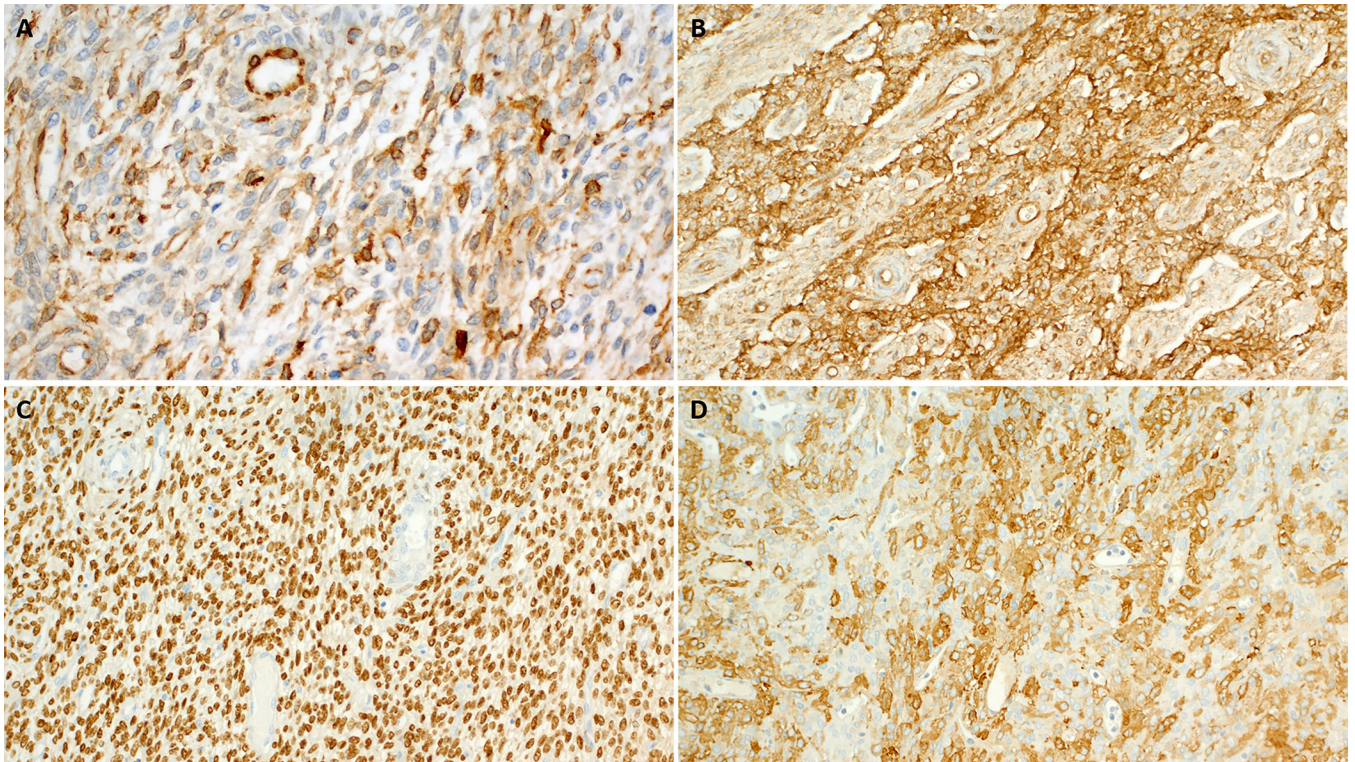
Representative images of the myxoid feature in *KAT6B::KANSL1* fusion sarcomas. **A:** Abrupt transition from moderately pink (myoid) areas to myxoid area. Note gradual merging of the myoid area (midfield) and more dark-stained areas (lower right). **B:** Focal epithelioid areas showing abrupt transition to arteriole-rich paucicellular myxoid area. **C:** Higher magnification of fibromyxoid spindled areas showing prominent vascularization. **D:** Prominent pericytoma-like vascular pattern.





**FIGURE 4.** Examples, of unusual features in *KAT6B::KANSL1* fusion sarcomas. **A+B:** Prominent sex cord-like pattern (note transition to striking myoid features in **A** upper right field). **C:** Small focus of hyaline collagenous spherules entrapping rounded primitive cells amid highly cellular sarcomatous background. **D:** Brightly eosinophilic collagen fibers as major stromal component are seen focally. **E:** This single example of sarcomatous highly pleomorphic tumor shows transition from spindled fascicular growth to undifferentiated epithelioid small round cell morphology. **F:** This case shows alternating fascicles of dark-stained smaller cells and moderately eosinophilic (myoid) spindled cells.



**FIGURE 5.**

Representative images of the immunohistochemical findings in *KAT6B::KANSL1* fusion sarcomas. **A:** Variable CD10 expression is noted. **B:** Strong and diffuse CD10 expression is seen in this case with sex cord like features. **C:** Homogenous expression of estrogen receptor. **D:** Moderate cytoplasmic expression of smooth muscle actin is seen in this case with *KAT6A::KANSL1* fusion.

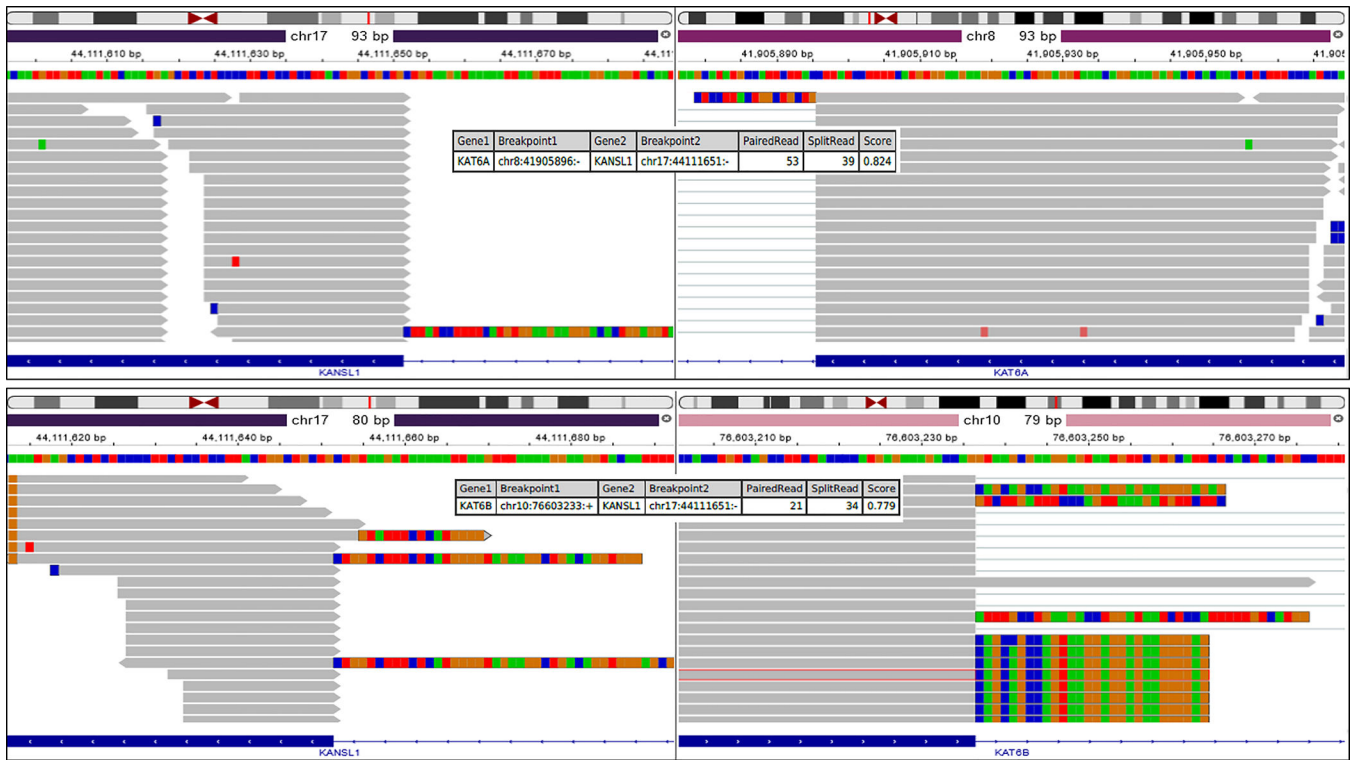


**FIGURE 6.** Integrated Genome Viewer (IGV) split-screen view of read alignments of the identified *KAT6A::KANS1* (upper picture; Case 2) and *KAT6B::KANS1* (lower picture; Case 3) fusion event. Shown are the breakpoints in the *KAT6A* and *KAT6B* locus (left) and the *KANS1* locus (right), respectively. Alignments whose mate pairs are mapped to the fusion sequence are multi-colored (soft clips).

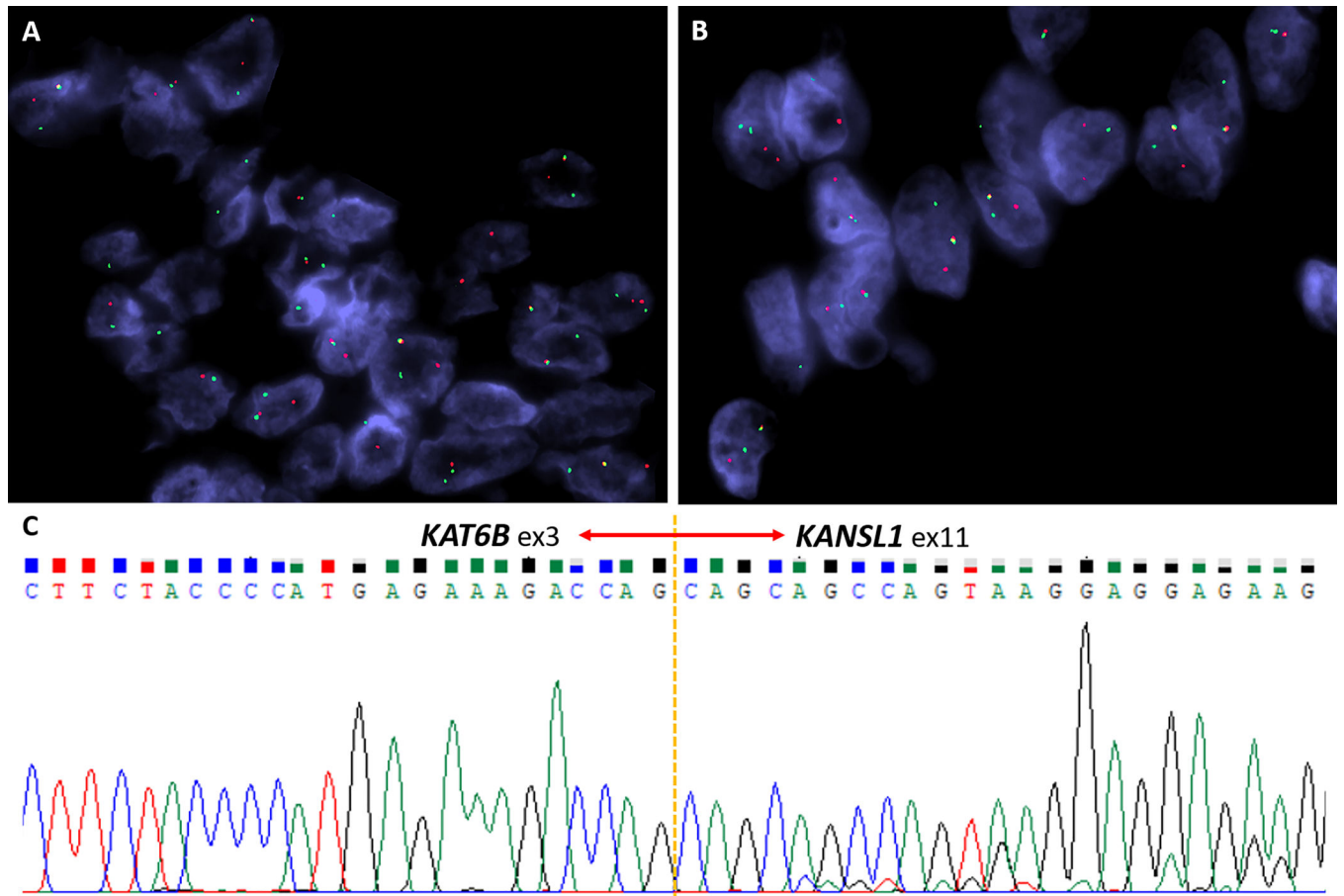


**FIGURE 7.** Representative images of fluorescence in situ hybridization (FISH) in Case 1 showing break-apart signals (indicated by arrowheads) in both *KAT6B* (**A**) and *KANSL1* (**B**). Red, centromeric; green, telomeric. **C:** RT-PCR confirming *KAT6B::KANSL1* fusion in Case 10.

**Table 1:** Clinicopathological features of *KAT6B/A::KANSL1* fusion-positive uterine sarcomas.

No	Age	Size cm	Original diagnosis	Treatment	Outcome (duration)
1	47	9	LG-ESS with limited CD10	Enucleation, then TAH-BSO	NED (23 mo)
2	63	NA	LG-ESS with aberrant diffuse cyclinD1	Curettage 2003 & 2020	Persistent disease (17 yrs)
3	34	5	LG-ESS	Hysterectomy	NED (10 mo)
4	46	2.6	LG-ESS	TAH-BSO	NED (9 mo)
5	50	7.5 + 15	LG-ESS with progression to HG-ESS	TAH-BSO	DOD (10 mo)
6	81	13	Initially LG-ESS, then changed to STUMP after molecular result	Hysterectomy	NED (34 mo)
7	58	12.5	LG-ESS with sex cord-like differentiation	TAH	AWD (24 mo)
8	40	6.5	Favor LG-ESS	Curettage	Recent case
9	53	2.7	Leiomyosarcoma	TAH-BSO	Synchronous lung metastases, DOD (<2 mo)
10	49	23.5	Infarcted leiomyoma (later considered myxoid leiomyosarcoma)	TAH-BSO, bilateral pelvic lymphadenectomy, omental biopsy	Lung metastasis (46 mo) DOD (47 mo)
11	39	N/A	Initially UTROSCT, subsequently LG-ESS with myoid features in the 1 <sup>st</sup> recurrence, and a cellular leiomyoma in the 2 <sup>nd</sup> recurrence	Myomectomy, TAH-BSO and debulking for recurrence	Bulky multinodular recurrence with extensive invasion of the uterine wall, polypoid projections in pelvic cavity & massive peritoneal sarcomatosis 7 yrs later, 2 <sup>nd</sup> & 3 <sup>rd</sup> recurrences 1.5 yrs & 9.5 yrs later, AWD 17 yrs after 1 <sup>st</sup> diagnosis
12	62	10	Undifferentiated uterine sarcoma with nuclear uniformity	TAH-BSO	NED (6 mo)
13	33	N/A	LG-ESS vs. HG-ESS	Myomectomy, then TAH-BSO	Recent case

AWD=alive with disease; BSO=bilateral salpingo-oophorectomy; DOD=died of disease; HG-ESS=high-grade endometrial stromal sarcoma; LG-ESS=low-grade endometrial stromal sarcoma; NA=not available; NED=no evidence of disease; STUMP=smooth muscle tumor of unknown malignant potential; TAH=total abdominal hysterectomy.



Gross and microscopic findings in *KAT6B/A::KANSL1* fusion positive uterine sarcomas

Table 2:

No	Tumor location	Peripheral border	Predominant histology	Sex cord-like features	Myxoid change	Hyaline collagen deposits	Eosinophilic myoid cells	Necrosis	Mitoses/10 hpf
1	Myometrial	Well-circumscribed	LG-ESS-like	Present	Present	Absent	Absent	Present	22
2	Endometrial	Not assessable (curettage)	LG-ESS-like	Absent	Absent	Absent	Absent	Absent	1
3	Myometrial	Well-circumscribed	LG-ESS-like	Present	Present	Present	Absent	Absent	12
4	Myometrial	Infiltrative	LG-ESS	Absent	Present	Present	Present	Absent	3
5	(A) Myometrium (B) Broad ligament	(A) Well-circumscribed (B) Not assessable (disrupted)	(A) LG-ESS-like (B) Biphasic undifferentiated	(A) Absent (B) Absent	(A) Absent (B) Present	(A) Present (B) Present	(A) Present (B) Present	(A) Present (B) Present	(A) 2 (B) >20
6	Myometrial	Well-circumscribed	LG-ESS-like	Absent	Present	Absent	Present	Present	1
7	Intracavitary, protruding through cervical canal, extending to outer 1/3 of myometrium	Well-circumscribed	LG-ESS-like	Present	Present	Present	Absent	Present	3
8	Myometrial	Well-circumscribed (radiologically)	LG-ESS-like	Absent	Absent	Present	Present	Absent	2
9	Myometrial	Infiltrative	Undifferentiated spindle-epithelioid cells	Absent	Present	Absent	Absent	Present	>20
10	Myometrial	Well-circumscribed, focal myometrial entrapment	Fibromyxoid variant of LG-ESS-like	Present	Present	Present	Present	Present	3
11	Myometrial	Well-circumscribed	LG-ESS-like	Present	Present	Present	Present	Present	8
12	Myometrial	Well-circumscribed	Sex cord-like	Present	Absent	Present	Present	Present	16
13	Myometrial with exophytic polypoid component	Infiltrative with myometrial vascular involvement	LG-ESS-like	Absent	Absent	Absent	Absent	Present (extensive)	2

LG-ESS=low-grade endometrial stromal sarcoma; N/A=not available.



**Table 3:** Immunohistochemical findings in *KAT6B/A::KANSL1* fusion positive uterine sarcomas

No	Desmin	SMA	h-CD	CD10	CyclinD1	ER	PR	Calretinin	Inhibin	CK	WT1
1	-	+	-	-	-	++	+++	-	-	-	-
2	-	++	-	+++	+++	+++	+++	-	-	-	-
3	-	+	-	+++	-	++	+++	-	-	-	-
4	-	-	-	+++	-	N/A	N/A	N/A	N/A	N/A	N/A
5	++	N/A	N/A	+++	N/A	N/A	N/A	++	+	++	+++
6	-	++	-	+	-	+++	+++	N/A	N/A	-	N/A
7	N/A	N/A	N/A	+++	++	+++	+++	++	-	++	+
8	+	+++	+	+++	+	+++	+++	N/A	N/A	++	+++
9	-	+	-	+	++	-	-	N/A	N/A	N/A	N/A
10	-	++	+	+	-	-	-	N/A	N/A	N/A	N/A
11	+++	+	N/A	+	N/A	+++	+++	+	-	-	N/A
12	-	-	-	+	-	-	-	-	N/A	+	N/A
13	+	+	-	+++	+	+++	+++	-	-	+	+++

+ =<25%, ++=25-50%, +++=>50%, h-CD: h-caldesmon, N/A: not available

**Table 4:**

Breakpoints of the *KAT6B/A::KANSL1* fusions in uterine sarcomas

No	RNA fusion results	Breakpoints <i>KAT6B/A</i>	Breakpoints <i>KANSL1</i>
1	<i>KAT6B::KANSL1</i>	NM_012330.4; exon 3 of 18 of <i>KAT6B</i>	NM_001193466.2; exon 11 of 15
2	<i>KAT6A::KANSL1</i>	NM_006766.5; exon 2 of 17 of <i>KAT6A</i>	NM_001193466.2; exon 11 of 15
3	<i>KAT6B::KANSL1</i>	NM_012330.4; exon 3 of 18 of <i>KAT6B</i>	NM_001193466.2; exon 11 of 15
4	<i>KAT6B::KANSL1</i>	NM_012330.4; exon 3 of 18 of <i>KAT6B</i>	NM_001193466.2; exon 11 of 15
5	<i>KAT6B::KANSL1</i>	NM_012330.4; exon 3 of 18 of <i>KAT6B</i>	NM_001193466.2; exon 11 of 15
6	<i>KAT6B::KANSL1</i>	NM_012330.4; exon 3 of 18 of <i>KAT6B</i>	NM_001193466.2; exon 11 of 15
7	<i>KAT6B::KANSL1</i>	NM_012330.4; exon 3 of 18 of <i>KAT6B</i>	NM_001193466.2; exon 11 of 15
8	<i>KAT6B::KANSL1</i>	NM_012330.4; exon 4 of 18 of <i>KAT6B</i>	NM_001193466.2; exon 11 of 15
9	<i>KAT6B::KANSL1</i>	NM_012330.4; exon 4 of 18 of <i>KAT6B</i>	NM_001193466.2; exon 11 of 15
10	<i>KAT6B::KANSL1</i>	NM_012330.4; exon 3 of 18 of <i>KAT6B</i>	NM_001193466.2; exon 11 of 15
11	<i>KAT6B::KANSL1</i>	NM_012330.4; exon 3 of 18 of <i>KAT6B</i>	NM_001193466.2; exon 11 of 15
12	<i>KAT6A::KANSL1</i>	NM_006766.5; exon 2 of 17 of <i>KAT6A</i>	NM_001193466.2; exon 11 of 15
13	<i>KAT6B::KANSL1</i>	NM_001370139; details of exons not available	NM_001193466.2; exon 11 of 15